

# Estimating lung volume during high frequency ventilation

S. L. Waters<sup>1</sup>, O. E. Jensen<sup>2</sup>, J. A. D. Wattis<sup>2</sup>, & J. Ahluwalia<sup>3</sup>

<sup>1</sup> DAMTP, University of Cambridge, Silver Street, Cambridge CB3 9EW

<sup>2</sup> Division of Theoretical Mechanics, School of Mathematical Sciences,  
University of Nottingham, University Park, Nottingham NG7 2RD

<sup>3</sup> Rosie Maternity Hospital, Addenbrooke's NHS Trust, Robinson Way, Cambridge CB2 2SW

February 2001

## Introduction and Aims

The primary goals of lung ventilation are to bring oxygen into the alveoli from where it can enter the blood, and to eliminate carbon dioxide dissolved in the blood. Since  $\text{CO}_2$  is much more soluble in blood than oxygen,  $\text{O}_2$  transport is diffusion-limited and a large alveolar surface area is the primary factor controlling its delivery.  $\text{CO}_2$  transport is flow-limited, so that efficient gas transport and mixing in the lung primarily controls its elimination from the blood.

The lung has approximately 20 generations of bifurcating airways which terminate in elastic sacs known as alveoli, where the majority of gas exchange occurs. During inspiration, the volume of the thoracic cavity increases and air is drawn into the lung. The lung is elastic and returns passively to its pre-inspiratory volume during expiration. Figure 1 shows a pressure-volume curve for a lung, which may be found using the apparatus shown on the left of figure 1. When the pressure within the jar is reduced below atmospheric pressure, the lung expands and its volume change can be measured. The quasi-static pressure-volume curves for inflation and deflation are different. This hysteresis arises in part from the effects of surface tension of the thin liquid film lining the airways of the lung. The slope of the pressure-volume curve (volume change per unit pressure change) is known as the compliance. The lung has low compliance at high lung volumes.

Artificial ventilators are often used to support premature infants suffering from respiratory distress, which is often associated with a deficiency of pulmonary surfactant. Under Conventional Mechanical Ventilation (CMV), which operates at normal tidal frequencies, the lungs are actively inflated at each breath, and they recoil passively to expel inhaled air. A clinician can control six ventilator variables:

- the Peak Inflation Pressure (PIP, typically 20 cm  $\text{H}_2\text{O}$ ),
- the Positive End Expiratory Pressure (PEEP, typically 5 cm  $\text{H}_2\text{O}$ )
- the inspiration and expiration time ( $T_i$  and  $T_e$ ) which determines the frequency  $f$  (typically 60 cycles/min),
- the mean-flow-rate of the ventilator  $Q$ ,

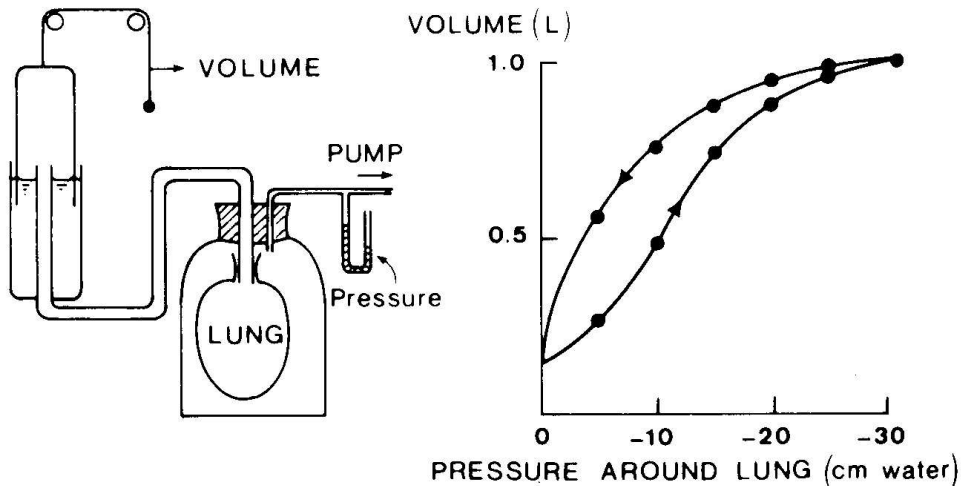


Figure 1: Measurement of the pressure-volume curve of excised lung. The lung is held at each pressure for a few seconds while its volume is measured. The curve is nonlinear and becomes flatter at higher expanding pressures. The inflation and deflation curves are not the same (hysteresis) (from [9]).

- the fraction of inspired  $O_2$  in the air supply ( $FiO_2$ ).

Increasing the difference  $PIP-PEEP$  increases the tidal volume  $VT$  (the volume of air entering the lung during each breath). The efficiency of  $CO_2$  elimination is approximately proportional to the product  $VT \times f$ , although excessively rapid, large-amplitude breaths can be traumatic to airways. Raising  $PEEP$  keeps airways inflated at the end of each breath, preventing small airways and alveoli from collapsing, and ensuring good  $O_2$  exchange in alveoli. If  $PIP$  is too high there is a danger the lungs will overdistend, adversely affecting  $VT$  and  $CO_2$  clearance (and, through *barotrauma*, potentially causing chronic lung disease). The effectiveness of ventilation can be measured by the continuous monitoring of  $CO_2$  levels in the blood, hot-wire measurements of  $VT$  in the endotracheal tube and visual assessments of chest wall movements. These observations guide the clinician in setting the appropriate value of  $PIP$ ,  $PEEP$ ,  $Ti$  and  $Te$ ,  $Q$  and  $FiO_2$ .

When  $CMV$  fails, High Frequency Ventilation ( $HFOV$ ) may be used. Under  $HFOV$ , the ventilator variables that can be controlled are the mean airway pressure ( $MAP$ , typically 15 cm  $H_2O$ ), the frequency of the oscillations  $f$  (typically around 10 Hz, which is comparable to the resonant frequency of the lungs), the pressure amplitude of the pump oscillator ( $P_{amp}$ ) and  $FiO_2$ . In this case, inspiration and expiration are both actively controlled by the pump. Although  $P_{amp}$  is large (roughly 40 cm  $H_2O$ ), the resulting pressure fluctuations in the alveoli are smaller, and they fall in magnitude as  $f$  is increased in a manner controlled by the resistance and compliance of the lungs and of the ventilator itself. The tidal volume  $VT$  is also small, and it too falls as  $f$  is increased.  $MAP$  controls the mean lung distension: this should be large enough for small airways to be recruited, but not so large that lung compliance falls because airways become overdistended.  $O_2$  delivery is therefore controlled primarily by  $MAP$  and  $FiO_2$ .  $CO_2$  elimination is controlled by the degree of mixing in the airways, and it correlates approximately with  $VT^2 \times f$ ; for a review of the various mechanisms of gas mixing and transport that are thought to operate during  $HFOV$  see [2]. Continuous measurements of  $CO_2$  levels in the blood,  $VT$  and a pressure measurement at the ventilator are available to the clinician, as are occasional measurements of lung volume  $V$  by X-ray, but X-rays are

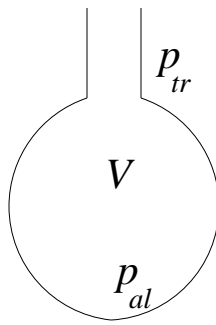


Figure 2: Simple one-compartment lung model.

inaccurate and potentially harmful. An alternative technique for estimating  $V$  is sought.

One possible method uses *respiratory inductance plethysmography*, which has recently been validated against whole-body plethysmography [8]. Here we wish investigate whether  $V$  can instead be assessed directly from the data available from the ventilator. To do this, we develop a simple lumped-parameter model of the system. We find that, while direct estimation of  $V$  is difficult, we can determine the lung compliance, at least in principle. Ideally ventilation should occur in the regime where the compliance is greatest so that the least possible damage is done to the airways. We shall also determine how the pressure fluctuations, initially of size  $P_{amp}$ , are attenuated through the system resulting in smaller pressure fluctuations at the alveoli.

### Simple lung model - without ventilator

We start by considering a very simple model, whereby the lung is assumed to be comprised of a single compartment containing the large airways and all other lung tissue (Figure 2). Its mechanical properties are characterised by

$$p_{al} - P(V) = DV_t, \quad (1)$$

$$p_{tr} - p_{al} = R_{aw}V_t + I_{aw}V_{tt}, \quad (2)$$

where  $p_{tr}$  is the tracheal pressure,  $p_{al}$  is the alveolar pressure,  $V$  is the lung volume (typically in the range 20-40 ml/kg) and the subscript  $t$  denotes a time derivative.  $R_{aw}$  is the airway resistance,  $I_{aw}$  is the airway inertance,  $P(V)$  is the quasi-static pressure-volume relation for the lung and  $D$  represents lung tissue damping. We assume  $P(V)$  is a single-valued function, even though for large excursions it exhibits hysteresis (Figure 1). Equation (1) is the ‘wall law’ or ‘tube law’ for the lung tissue and equation (2) relates the pressure drop across the lung to the resistance and inertance of the system. We are neglecting nonlinearities in airway resistance, such as the fact that expiratory resistance is typically four times greater than inspiratory resistance [7]. This simple linear model is equivalent to that used in [4], where the analogous electrical circuit is described.

To model small-amplitude, oscillatory ventilation, we consider  $V$  and the pressures to consist of a steady and a time-dependent part as follows:

$$V = V_0 + \Re(V_1 e^{i\omega t}), \quad (3)$$

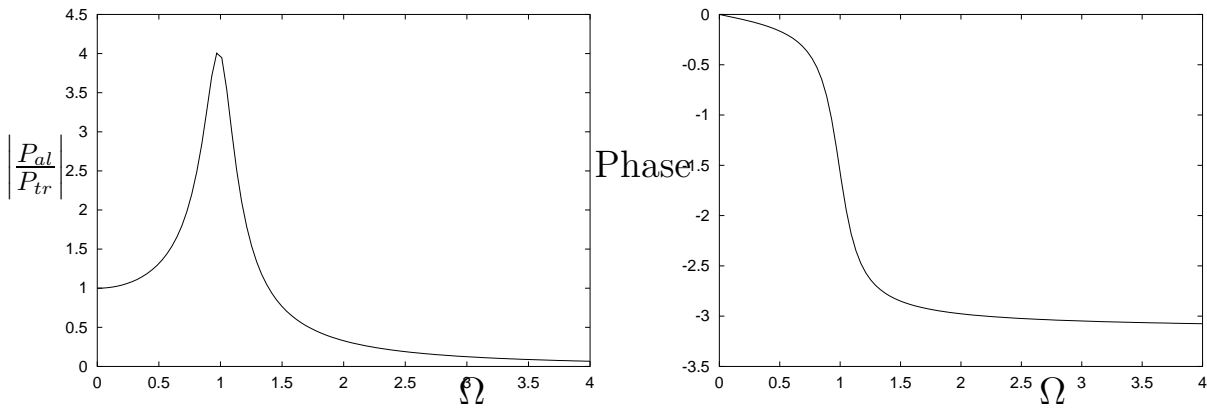


Figure 3: (a)  $|P_{al}/P_{tr}|$  versus  $\Omega$ ; (b) Phase of  $P_{al}/P_{tr}$  versus  $\Omega$ . ( $\delta = 0.25$ )

$$p_{al} = P(V_0) + \Re(P_{al}e^{i\omega t}), \quad (4)$$

$$p_{tr} = P(V_0) + \Re(P_{tr}e^{i\omega t}), \quad (5)$$

where  $\omega$  is the frequency of the system,  $P_{al}$  and  $P_{tr}$  are complex amplitudes and the amplitude  $V_1$  is real. Substituting (3–5) into (1) and (2) gives

$$P_{al} - P'(V_0)V_1 = i\omega DV_1, \quad (6)$$

$$P_{tr} - P_{al} = R_{aw}i\omega V_1 - \omega^2 I_{aw}V_1, \quad (7)$$

from which we obtain the following expression for the ratio  $P_{al}/P_{tr}$ :

$$\frac{P_{al}}{P_{tr}} = \frac{E + i\omega D}{E + i\omega(D + R_{aw}) - \omega^2 I_{aw}}, \quad (8)$$

where  $E = P'(V_0)$  is the lung elastance ( $1/E$  is the static compliance, which is in the range 0.4 to 0.5 ml/cm H<sub>2</sub>O/kg for newborn infants [5]). The system exhibits a damped resonance with resonant frequency  $\omega_r^2 = E/I_{aw}$ . If we assume  $D \ll R_{aw}$  (which is reasonable according to [3]; see [6]) and non-dimensionalise using

$$\Omega = \frac{\omega}{\omega_r}, \quad \delta = \frac{\omega_r R_{aw}}{E}, \quad (9)$$

where  $\delta$  is a dimensionless measure of the damping of the system, we get

$$\frac{P_{al}}{P_{tr}} = \frac{1}{(1 - \Omega^2) + i\Omega\delta}. \quad (10)$$

Figure 3a shows  $|P_{al}/P_{tr}|$  against  $\Omega$  for  $\delta = 0.25$ . In general, the resonance peak is of height  $1/\delta$  and the width of the peak is  $\mathcal{O}(\delta)$ . Figure 3b shows the phase of  $P_{al}/P_{tr}$  which tends to  $-\pi$  as  $\Omega$  becomes large. Experimental evidence for resonance in the lung may be found in [4] (excised dog lung), [1] (excised rabbit lung) and [6] (healthy human lungs under forced oscillation). Estimates of the resonant frequency in healthy adults give  $\omega_r \sim 8 - 13\text{Hz}$  [6].

## Estimating Elastance and Inertance

From equations (3)-(7) we can relate the flow-rate into the lung  $Q_{tr}$  to the tracheal pressure, through

$$Q_{tr} = V_t = \Re[i\omega V_1 e^{i\omega t}] , \quad (11)$$

$$P_{tr} = \Re[V_1 (P'(V_0) + i\omega(D + R_{aw}) - \omega^2 I_{aw}) e^{i\omega t}] . \quad (12)$$

Assuming, as before,  $D \ll R_{aw}$  and non-dimensionalising according to (9) together with  $T = \omega_r t$ , we obtain

$$Q_{tr} = -V_1 \omega_r \Omega \sin \Omega T , \quad (13)$$

$$P_{tr} = V_1 E [(1 - \Omega^2) \cos \Omega T - \delta \Omega \sin \Omega T] . \quad (14)$$

In the limit as  $\delta \rightarrow 0$ , a plot of  $Q_{tr}$  against  $P_{tr}$  (assuming measurements of each are available) will give (according to this model) an ellipse with semi-axes  $X = V_1 \omega_r \Omega$  and  $Y = V_1 E(1 - \Omega^2)$ , separated by an angle  $(\pi/2) - \tan^{-1} \delta$ . Thus measurements of

$$\frac{X}{Y} = \frac{\omega}{E - I_{aw}\omega^2} \quad (15)$$

over a range of frequencies  $\omega$  will provide estimates of the lung elastance,  $E$ , and the airway inertance,  $I_{aw}$ . Hence, although  $V$  has not been assessed directly, lung compliance (given by  $1/E$ ) can be estimated. It would then be possible to see how compliance changes with MAP (or with time as lung properties change), so that the optimum compliance may be obtained.

## Lung model - with ventilator

We now include the effects of the ventilator and the endotracheal tube, again within the framework of a linear theory. Figure 4 shows a sketch of the apparatus. In the absence of imposed oscillations, a mean flow  $Q$  is driven through the system, exiting through a valve (with resistance  $R_V$ ) and possibly through a leak between the endotracheal (ET) tube and the trachea (resistance  $R_L$ , although the fact that air is leaking between the end of the endotracheal tube and wet, deformable airway walls suggests that the leak may not have linear pressure-flow characteristics, even at small amplitudes). The resistances of the ventilator tubing ( $R_2, R_3$ ) and of the ET tube  $R_{ET}$  control the steady pressure distribution  $p_1 > p_2 > p_3$ ,  $p_2 \geq p_{tr}$ . The value of  $p_{tr}$  controls mean lung inflation, and sets the mean airway pressure (MAP). Superimposed on this steady flow is an oscillatory flow driven by pressure fluctuations  $p_I$ . These are attenuated through the system and lead to small amplitude fluctuations in lung volume.

The full governing equations are

$$q_0 + Q = q_1 , \quad (16)$$

$$q_2 = q_3 + q_{ET} , \quad (17)$$

$$q_{ET} = V_t + q_L , \quad (18)$$

$$C p_{1t} = q_1 - q_2 , \quad (19)$$

$$p_I - p_1 = R_0 q_0 + I_0 q_{0t} , \quad (20)$$

$$p_1 - p_2 = R_2 q_2 + I_2 q_{2t} , \quad (21)$$

$$p_2 - p_3 = R_3 q_3 + I_3 q_{3t} , \quad (22)$$

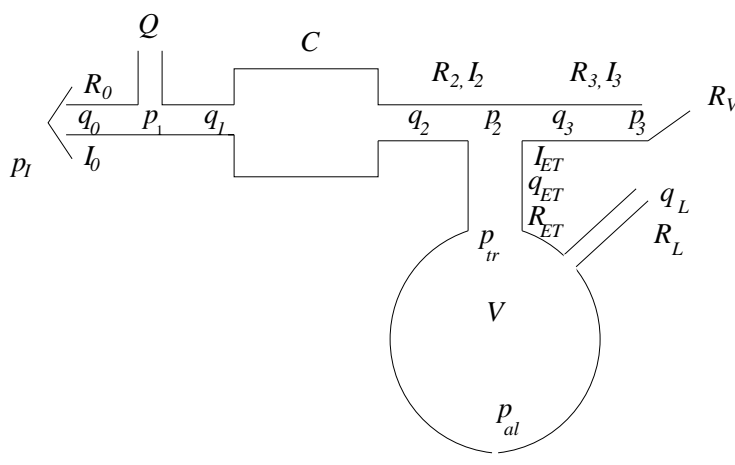


Figure 4: Model of lung together with ventilator and endotracheal tube.

$$p_2 - p_{tr} = R_{ET}q_{ET} + I_{ET}q_{ETt} , \quad (23)$$

$$p_3 = R_V q_3 , \quad (24)$$

$$p_{tr} = R_L q_L , \quad (25)$$

$$p_{al} - P(V) = DV_t , \quad (26)$$

$$p_{tr} - p_{al} = R_{aw}V_t + I_{aw}V_{tt} , \quad (27)$$

where  $p_i$ ,  $I_i$ ,  $R_i$ ,  $q_i$  denote pressure, inertance, resistance and flow rate respectively.  $C$  represents ventilator compliance.  $V(t)$  is again lung volume and  $D$  lung damping (see figure 4).

Once again we let

$$V = V_0 + V_1 e^{i\omega t} , \quad q_i = q_i^s + Q_i e^{i\omega t} \quad (28)$$

$$p_I = p_I^s + P_{amp} e^{i\omega t} , \quad p_{al} = p_{al}^s + P_{al} e^{i\omega t} , \quad p_{tr} = p_{tr}^s + P_{tr} e^{i\omega t} , \quad p_i = p_i^s + P_i e^{i\omega t} \quad (29)$$

(real parts assumed), where superscripts  $s$  denote the steady component. By solving the resulting system of simultaneous equations for the complex amplitudes, we are able to determine  $P_{al}/P_{amp}$ . Suppose, for simplicity, we neglect  $R_2, R_3, I_2, I_3, I_{ET}, I_0, R_0$  and  $R_L$ , but assume that the compliance,  $C$ , is sufficiently large that we keep terms  $CR_0$ . We then obtain the following expression for  $P_{al}/P_{amp}$ :

$$\frac{P_{al}}{P_{amp}} = \frac{E + i\omega D}{(1 + Ci\omega R_0) \left[ \left(1 + \frac{R_{ET}}{R_L}\right) (i\omega R_{aw} + E + Di\omega - \omega^2 I_{aw}) + i\omega R_{ET} \right]} . \quad (30)$$

If we non-dimensionalise according to (9), setting  $C = CR_0\omega_r$ , and assume as before that  $D \ll R_{aw}$ , we get

$$\frac{P_{al}}{P_{amp}} = \frac{1}{(1 + C\Omega i) \left( (1 - \Omega^2) + i\delta\Omega + i\Omega\delta\frac{R_{ET}}{R_{aw}} \right)} . \quad (31)$$

Thus we see that the ventilator compliance and the endotracheal tube resistance both contribute to the attenuation of the pressure peak.

Similarly, we can obtain expressions for tidal volume and pressure measured at the ventilator, analogous to (13, 14). These quantities are recorded automatically by the ventilator (at least by the Dräger BabyLog model used in the Rosie Hospital, Cambridge). Fitting pressure-flow loops to the theoretical expressions should enable us to determine lung compliance, as described in §.

## Experiment

To investigate these ideas further, a simple experiment was conducted at the Rosie Maternity Hospital, Cambridge, a few weeks after the study group. A Dräger Babylog ventilator was connected to a model lung (an inflatable plastic bottle). Pressure-volume loops were recorded over a range of frequencies. Pressures are measured within the ventilator; the recorded pressure is that inferred by the ventilator (through some unknown algorithm) to be the pressure at the level of the ET tube. Many loops were clearly nonlinear; at some parameter values, distinct oscillations were obtained depending on the manner in which the operating point was approached through parameter space. Some oscillations were highly irregular, and possibly chaotic. The complex dynamics may be driven in part by the control system within the ventilator.

For this preliminary study, we attempted to fit the linear model presented in Section 2 to the system. The system compliance was measured at low frequencies to be  $E \approx 1.74 \text{ cm H}_2\text{O}/\text{cm}^3$ . Pressure-volume graphs were measured at high frequencies (5–20 Hz), with a fixed oscillatory amplitude and a fixed mean airway pressure. An ellipse was fitted to each loop, and semi-major and semi-minor axes  $a^*$  and  $b^*$  were measured (in cm), along with  $\alpha^*$ , the angle of the major axis to the horizontal (pressure) axis. Knowing calibration scales  $L_p$  and  $L_v$  of each axis (in cm/cm H<sub>2</sub>O and cm/cm<sup>3</sup> respectively), and scaling volumes on an unknown scale  $V_1$  and pressures on  $V_1 E$ , the quantities

$$\frac{a}{b} = \frac{a^* \tan \alpha^*}{b^* \tan \alpha}, \quad \tan \alpha = \frac{E L_p}{L_v} \tan \alpha^*$$

provide scale-independent measurements of each experiment.

From (13,14), with  $X = P_{tr}/V_1 E$  and  $Y = V/V_1$ , we have

$$\frac{1}{\delta^2 \Omega^2} [X^2 - 2XY(1 - \Omega^2) + (1 - \Omega^2)^2 Y^2] + Y^2 = 1.$$

An ellipse with semi-axes  $a$  and  $b$ , tilted an angle  $\alpha$  to the horizontal in the  $(X, Y)$  plane is described by

$$X^2 \left( \frac{c^2}{a^2} + \frac{s^2}{b^2} \right) + 2XYcs \left( \frac{1}{a^2} - \frac{1}{b^2} \right) + Y^2 \left( \frac{s^2}{a^2} + \frac{c^2}{b^2} \right) = 1,$$

where  $c \equiv \cos \alpha$  and  $s \equiv \sin \alpha$ . Comparing coefficients gives three relations in these two expressions, we can deduce

$$\Omega^2 = 1 + \frac{\tan \alpha [1 - (a^2/b^2)]}{1 + (a^2/b^2) \tan^2 \alpha}$$

and likewise  $\delta^2$ . Since  $\omega$  is known, we may then deduce  $\omega_r$  and  $R_{aw}$ . Some results are presented in the table below.

$\omega$ (Hz)	$a/b$	$\alpha$ (degrees)	$\omega_r$ (Hz)	$R_{aw}$ (cm H <sub>2</sub> O s/cm <sup>3</sup> )
5	2.61	42	11.2	0.9
6	2.97	48	11.6	1.2
8	3.89	42	39.5	0.8
10	2.13	35	20.8	0.6
12	2.91	40	38.0	0.8
12	2.83	35 [125]	193.2 [23.5]	0.6 [0.4]
14	0.93	36	13.6	1.0
16	1.15	135	15.0	1.0
20	2.88	132	15.2	1.2

As the table of results shows, as the frequency is increased through 14 or 15Hz, the pressure-volume loops become round and then change orientation ( $\alpha$  increases above  $90^\circ$ ), as would be expected in going through a resonance. The predicted values of  $\omega_r$  are broadly consistent with this observation, in that  $\omega_r > \omega$  for  $\omega < 14\text{Hz}$  and  $\omega_r < \omega$  for larger frequencies.<sup>1</sup> However, the significant variation in  $\omega_r$  with frequency indicates major weaknesses in the simple model. Correspondingly, the model fails to predict a peak in the amplitude as a function of frequency near the probable resonance.

## Discussion

Our straightforward lumped-parameter model of the lung and ventilator captures dominant characteristics of lung behaviour, in particular resonance at certain frequencies. The model can in principle be used to predict lung compliance from measured pressure-flow curves. While the method does not measure lung volume directly, it can be inferred indirectly from the compliance. The practicality of this method is currently being investigated.

The large number of model parameters poses potential difficulties. The characteristics of the ventilator circuit should be quantifiable, although an open question concerns the appropriate method for determining and describing ventilator compliance: should this be in terms of tubing compliance or air compressibility? The air-leak from the end of the endotracheal tube, which is hard to quantify, may also be significant. The model can at least be used to estimate the sensitivity of the pressure-volume loops to the degree of leak. Future work will involve extending the current model in order to describe the experimental results more accurately.

## Acknowledgements

This report was prepared by Sarah Waters and Oliver Jensen (Nottingham). The following people also contributed to the work: Helen Byrne, Peter Howell, John King, David Riley (Nottingham), Tim Pedley (Cambridge), Jon Chapman (Oxford), John Billingham, Andy King (Birmingham), Marcus Tindall (Southampton).

## References

- [1] J. L. Allen, J. J. Fredberg, D. H. Keefe & I. D. Frantz, III (1985) Alveolar Pressure Magnitude and Asynchrony during High-Frequency Oscillations of Excised Rabbit Lungs. *Am. Rev. Resp. Dis.* **132**(2), 323–349.
- [2] H. K. Chang (1984) Mechanisms of gas transport during ventilation by high-frequency oscillation. *J. Appl. Physiol.* **56**, 553–563.
- [3] B.G. Ferris Jr, J. Mead & L.H. Opie (1964) Partitioning of respiratory flow resistance in man. *J. Appl. Physiol.* **19**, 653–658.
- [4] J. J. Fredberg, D. H. Keefe, G. M. Glass, R. G. Castile & I. D. Frantz, III (1984) Alveolar pressure nonhomogeneity during small-amplitude high-frequency oscillation. *J. Appl. Physiol.* **57**, 788–800.
- [5] E. Kelly, H. Bryan, F. Possmayer, H. Frndova & C. Bryan (1993) Compliance of the respiratory system in newborn-infants presurfactant and postsurfactant replacement therapy. *Pediatr. Pulmonol.* **15**, 225–230.

---

<sup>1</sup>Two measurements were taken at  $\omega = 12\text{ Hz}$ ; the second gives more reasonable predictions if  $\alpha$  is measured from the minor axis instead of the major axis.

- [6] R. Peslin & J. J. Fredberg (1986) Oscillation mechanics of the respiratory system. *In* Handbook of Physiology, Sec. III, Pt. 1, 2nd ed. Washington DC: American Physiological Society.
- [7] J.J. Pillow, H. Neil, M.H. Wilkinson & C.A. Ramsden (1999) Effect of I/E ratio on mean alveolar pressure during high-frequency oscillatory ventilation. *J. Appl. Physiol.* **87**, 407–414.
- [8] K. Weber, S. E. Courtney, K.H. Pyon, G.Y. Chang, P.B. Pandit & R.H. Habib (2000) Detecting lung overdistention in newborns treated with high-frequency oscillatory ventilation. *J. Appl. Physiol.* **89**, 364–372.
- [9] J. B. West (1995) Respiratory Physiology - the essentials. 5th Ed. Williams & Wilkins.